Review of Scientific Instruments

RESEARCH ARTICLE | OCTOBER 06 2022

M-STAR: Magnetism second target advanced reflectometer at the Spallation Neutron Source

Special Collection: New Science Opportunities at the Spallation Neutron Source Second Target Station

Valeria Lauter ; Kang Wang ; Tim Mewes ; Artur Glavic ; Boris Toperverg ; Mahshid Ahmadi ; Badih Assaf ; Bin Hu ; Mingda Li ; Xinyu Liu ; Yaohua Liu ; Jagadeesh Moodera ; Leonid Rokhinson ; Deepak Singh ; Nian Sun

Rev. Sci. Instrum. 93, 103903 (2022)
https://doi.org/10.1063/5.0093622

Review of Scientific Instruments ARTICLE scitation.org/journal/rsi

M-STAR: Magnetism second target advanced reflectometer at the Spallation Neutron Source

Cite as: Rev. Sci. Instrum. 93, 103903 (2022); doi: 10.1063/5.0093622
Submitted: 29 March 2022 • Accepted: 22 August 2022 •
Published Online: 6 October 2022

Valeria Lauter,[1,a)] Kang Wang,[2] Tim Mewes,[3] Artur Glavic,[4] Boris Toperverg,[5,6] Mahshid Ahmadi,[7] Badih Assaf,[8] Bin Hu,[7] Mingda Li,[9] Xinyu Liu,[8] Yaohua Liu,[10] Jagadeesh Moodera,[9] Leonid Rokhinson,[11] Deepak Singh,[12] and Nian Sun[13]

AFFILIATIONS

[1]Neutron Scattering Division, Neutron Sciences Directorate, Oak Ridge National Laboratory, 1 Bethel Valley Road, Oak Ridge, Tennessee 37831, USA
[2]Department of Electrical and Computer Engineering, Department of Physics, Department of Materials Science and Engineering, University of California, Los Angeles, California 90095, USA
[3]Magnetics Laboratory, Department of Physics and Astronomy, The University of Alabama, 1008 Bevill Bldg., Tuscaloosa, Alabama 3548, USA
[4]Laboratory for Neutron and Muon Instrumentation, Paul Scherrer Institut, 5232 Villigen PSI, Switzerland
[5]Department of Solid State Physics, Experimental Physics, Ruhr-University Bochum, Universitetsstrasse 150, Bochum D-44781, Germany
[6]Institut Laue Langevin, 6 rue Jules Horowitz, Grenoble 38042, France
[7]Department of Materials Science and Engineering, Institute for Advanced Materials and Manufacturing, University of Tennessee, 2641 Osprey Vista Way, Knoxville, Tennessee 37920, USA
[8]225 Nieuwland Science Center, University of Notre Dame, Notre Dame, Indiana 46556, USA
[9]Massachusetts Institute of Technology, 77 Massachusetts Ave., Bldg. 24-209, Cambridge, Massachusetts 02139, USA
[10]Second Target Station, Oak Ridge National Laboratory, 1 Bethel Valley Road, Oak Ridge, Tennessee 37831, USA
[11]Department of Physics, Purdue University, West Lafayette, Indiana 47906, USA
[12]223 Physics Building, Department of Physics and Astronomy, University of Missouri, Columbia, Missouri 65211, USA
[13]Electrical and Computer Engineering Department, Northeastern University, 360 Huntington Avenue, Boston, Massachusetts 02115, USA

Note: Paper published as part of the Special Topic on New Science Opportunities at the Spallation Neutron Source Second Target Station.
[a)]**Author to whom correspondence should be addressed:** lauterv@ornl.gov

ABSTRACT

M-STAR is a next generation polarized neutron reflectometer with advanced capabilities. A new focusing guide concept is optimized for samples with dimensions down to a millimeter range. A proposed hybrid pulse-skipping chopper will enable experiments at constant geometry at one incident angle in a broad range of wavevector transfer Q up to 0.3 A^{-1} for specular, off-specular, and GISANS measurements. M-STAR will empower nanoscience and spintronics studies routinely on small samples (~2 × 2 mm^2) and of atomic-scale thickness using versatile experimental conditions of magnetic and/or electric fields, light, and temperature applied *in situ* to novel complex device-like nanosystems with multiple buried interfaces. M-STAR will enable improved grazing incidence diffraction measurements, as a surface-sensitive *depth-resolved* probe of, e.g., the *out-of-plane* component of atomic magnetic moments in ferromagnetic, antiferromagnetic, and more complex structures as well as *in-plane atomic-scale structures* inaccessible with contemporary diffractometry and reflectometry. New horizons will be opened by the development of an option to probe near-surface dynamics with inelastic grazing incidence scattering in the time-of-flight mode. These novel options in combination with ideally matched parameters of the second target station will place M-STAR in the world's leading position for high resolution polarized reflectometry.

 https://doi.org/10.1063/5.0093622

I. INTRODUCTION

A. Key novel capabilities: Advancing the frontiers of knowledge

Polarized neutron reflectometry (PNR) is a depth-sensitive and nondestructive means to probe magnetic and structure profiles at the nanoscale for thin films and interfaces in quantum materials, spintronics, functional materials, soft matter, and biology.[1–5] PNR is uniquely able to probe phenomena at interfaces buried within materials.[6–11] Novel interfaces often yield new material properties or reveal new physical phenomena. There is a large user community in the field of quasi-2D magnetic structures, spintronics, and topological insulator heterostructures, which actively applies the method of PNR to a huge number of systems[12–15]

The application of neutron scattering for developments in fundamental science has significantly transformed our knowledge and technology. M-STAR will take advantage of over 20 times higher neutron flux of the STS than the world's leading first target station (FTS) at Spallation Neutron Source (SNS) and will become a next generation instrument capable of responding to new scientific and technological challenges.

1. High intensity and small sample size

Currently, a significant limitation of PNR is the required sample size. Equipment to carry out reflectometry experiments on *very small samples with sub-nanometer thickness and area of only* 1–2 mm^2 are often in demand by users; but, these experiments cannot be efficiently performed on existing reflectometers, inevitably preventing the application of this powerful method to scientific problems where sufficiently large samples are not available. A practical sample size on the order of 10 × 10 mm^2 is routinely used on contemporary polarized reflectometers. Slightly smaller samples require days—long measuring time—and can be measured in a very limited range of wavevector transfer due to a high background, resulting in insufficient quality of the acquired data. M-STAR will empower nanoscience and spintronics studies routinely on small samples (~2 × 2 mm^2) and of atomic-scale thickness using versatile experimental conditions of magnetic and/or electric fields, light, and temperature applied *in situ* to novel nanosystems and to complex device-like systems with multiple buried interfaces.

2. Broad wavelength band for time-of-flight (ToF) reflectometry, off-specular scattering (OSS), and grazing incidence small angle neutron scattering (GISANS)

The state of the art in surface preparation and characterization has made it feasible to produce new types of materials that are structured on the nanometer scale. Grazing-angle neutron scattering and properties of structures with reduced dimensionality in one direction are constantly developing fields of modern condensed-matter research. The development of advanced methods of thin film preparation has created an avalanche of demand for the characterization of thin film properties. At present, only conventional specular reflectometry (SR) is commonly used to investigate the structure of films or multilayers perpendicular to their surfaces, with fields of application ranging from magnetic multilayers to biological films. SR delivers information about the depth profile of the mean scattering length density (SLD) averaged over the whole sample surface. However, in reality, pure SR does not exist because real surfaces or interfaces are not ideal and cannot be atomically flat, while thin films are not perfectly homogeneous. Therefore, SR is always accompanied by off-specular scattering (OSS).[16–22] The latter probes the lateral structure (lateral form-factor, structure factor and/or the roughness, and magnetic and structural domains). Thus, the most exhaustive and detailed information on the three-dimensional structure (transverse and lateral) of multilayers can be gained using a combination of grazing incidence neutron or x-ray scattering techniques, comprising SR and OSS.[23–26] However, the high repetition rate of the FTS results in a short wavelength band, which makes it impossible to measure the reflectivity of a sample at a constant geometry, the main advantage of ToF SR.[27] For example, the measurement of reflectivity in the range of wavevector transfer up to 0.25 A^{-1} at 60 Hz repetition rate for the $2.6 < \lambda < 5.6$ A wavelength band requires up to six scattering angles, and up to four angles are required for $2.6 < \lambda < 8.6$ A at 30 Hz repetition rate.[25] This results in the necessity for stitching data of multiple measurements carried out at different incident angles α_i and, hence, at different illumination conditions. Moreover, the main problem is in merging the two-dimensional maps of the OSS. In OSS, the same overlapping Δq-range measured for two consecutive angles—is measured with two limiting wavelengths (λ_{min} and λ_{max}) of the spectrum, which results in stitching of the data measured with different resolutions and coherence lengths. M-STAR will enable experiments at a constant geometry at one incident angle, resulting in a broad range of wavevector transfer Q up to 0.3 A^{-1} for SR, OSS, and GISANS measurements. In combination with a high intensity, these measurements will be possible even for very small samples, which will considerably increase the application of neutron reflectometry by modern centers of excellence for nanoscience and nanotechnology.

3. Depth-sensitive grazing incidence diffraction

M-STAR will establish unique world-class capabilities for magnetic surface-sensitive grazing incidence diffraction (GID), which will constitute a *depth-resolved* probe of the *out-of-plane* component of atomic magnetic moments in ferromagnetic, some antiferromagnetic, and more complex structures as well as the *in-plane atomic-scale structures* inaccessible with up-to-date diffractometry and reflectometry.[28,29] One cannot overstate the importance and the novelty of this development. Conventional 3D powder, or single crystal diffractometers, such as CORRELI at SNS and that proposed for the STS VERDI and PIONEER, operate in the Laue diffraction ToF mode in the regime of the so-called "wide-angle" atomic-scale diffraction, showing rather high luminosity and ability to record single crystal diffraction and diffuse scattering from small single

crystals and even from relatively thin (down to ~0.1 μm) epitaxial films, probing the crystal structure averaged over their volume, whose shape, due to kinematics, does not play a role. The depth sensitivity is lost in conventional wide-angle diffractometry (WAD) and cannot be compensated for by its ability to provide information on three-dimensional atomic and magnetic arrangement averaged over the film volume and independent of boundary conditions at surfaces and interfaces. The way out assumes an implementation in the M-STAR reflectometer of an additional operation mode specialized for GID measurements. This option naturally combines diffractometry with reflectometry, using the same beam-forming and polarization setup, as well as the advantages of the ToF mode. M-STAR will be equipped with one or several additional position-sensitive detectors placed to record the lateral Bragg diffraction into angles in the horizontal plane. In contrast to WAD, GID is a depth-sensitive technique utilizing the entire wavelength band available and is, thus, capable of measuring, for example, larger magnetic structures (e.g., helical, spiral). Depth sensitivity of lateral atomic-scale diffraction occurring at large in-plane Bragg angles will be achieved via recording the Bragg peak intensity variation as a function of the small wavevector transfer component normal to the surface. The latter is measured at a fixed angle of incidence via the ToF method simultaneously with SR.

4. Grazing incidence inelastic scattering

New horizons will be opened by the development of additional capabilities of M-STAR to probe near-surface dynamics with grazing incidence inelastic scattering (GIINS) in the ToF mode. For many decades, neutron spectroscopy has been recognized as one of the most powerful tools for studying thermal excitations, or more generally, atomic and spin dynamics in condensed matter, delivering detailed and fundamental information over a wide range of scales in time and space. This became possible due to the presence of a large number of different types of spectrometers at all the leading neutron facilities in the world. At the same time, there are almost no instruments dedicated to probe surface and/or thin film dynamics, both intrinsic and induced by external time-dependent field.[30,31] Meanwhile, several recent experiments carried out, for example, on lipid bilayers stacked in periodic multilayers have unambiguously demonstrated the ability of neutron triple-axes spectroscopy to address some of the most intriguing questions on the co-operative dynamics of bio-mimetic membranes.[32] Despite the obvious success of this benchmark and other subsequent experiments, one should admit that this kind of spectrometry is not ideal for studying surface and thin film dynamics, e.g., due to its relatively low luminosity and resolution. In this regard, a dedicated advanced GIINS option based on ToF OSS, ToF GISANS, or ToF GID will be developed to perform depth-sensitive inelastic scattering. The ability to measure GIINS will render new opportunities to access dynamics in complex layered systems, surface excitation spectra in liquids, polymers, biological membranes, and other substances.

B. Scientific challenges

Although a wide range of the user community from various scientific fields will significantly benefit from the new capabilities, some of the key and specific cases described below are currently not feasible to study using any of the existing reflectometers. M-STAR will enable the study of the structure and dynamics of surfaces and interfaces in unprecedented details, which are beyond the limits of the current instrumentation.

1. Novel quantum materials

An understanding of interfacial complex behavior, especially when two quantum systems are coupled, is essential for advancing the field of quantum materials. Structures' hybridizing topological insulators (TIs) or superconductors (SCs) with ferromagnets (FMs) are key platforms for enabling new quantum states, for investigating intriguing correlated interaction, due to the electrostatic and quantum mechanical nature of the exchange coupling prevailing at the proximitized interface. Aided by the exchange fields, TI and SC characteristics can be profoundly modified owing to time-reversal symmetry breaking, exchange gap opening in the Dirac surface states of TI, while triplet pairing and/or Majorana bound states occur in SCs. Fascinating physics emerges at the interface of ferromagnetic materials coupled to materials with high spin–orbit coupling (SOC). Due to exchange interaction between polarized spins and the magnetic moments at the interface of FM/high-SOC materials, the out-of-plane (OOP) magnetic anisotropy has been commonly observed in these heterostructures. These effects are magnified in materials with high SOC, such as topological insulators (TIs). Although PNR is an ideal technique to probe the magnetization depth profile in various types of thin film heterostructures at the nanometer scale,[5,33–39] there exist limitations in characterizing interfacial spin textures because of (a) the requirement for large sample dimensions and (b) an inability to probe the out-of-plane component of magnetization.[40] The GID capability proposed for M-STAR will enable measuring the depth profile of the perpendicular component of magnetization. In combination with the more conventional PNR method for obtaining the depth profile of an in-plane magnetization, M-STAR will provide a complete picture of the interfacial spin texture in TI/FM heterostructures.

The ability to focus the beam onto a small sample area will enable the study of dynamic effects in multilayered magnetic thin film heterostructures. For example, a small sample size of 2×2 mm^2 can be easily patterned to perform Inverse Spin-Hall Effect (ISHE) experiments. An RF field acting on a thin FM film causes precession of the magnetization, which, in turn, generates spin currents. A high-SOC material such as TI coupled to FM will convert the spin current to transverse charge current due to ISHE, which can be measured as a voltage signal across the sample. The ability to characterize the magnetization depth profile of these samples at resonance will make it possible to characterize the magnetization dynamics over the cross section of the sample. This would be immensely beneficial for the design and development of robust spintronic memory and logic devices. Such studies cannot be performed on current instruments due to sample size limitations, limited wavelength band, and low intensity.

2. Topological insulator heterostructures—science of interfaces and quasiparticles

Recent theoretical developments have accelerated the prediction of novel quantum phases. Some newly predicted phases are metastable or predicted in heterogeneous structures that can be

stabilized by epitaxial growth. Due to the lack of commercial substrates isostructural to many of the predicted materials, there is a trend to grow films on single crystal substrates, which are often as small as 2 × 2 mm^2—too small for routine measurements on current instruments. The ability of M-STAR to measure samples of this size will remove this limitation and enable the study of phase transitions in heterostructures and superlattices, their response to external fields, and the creation of new quasiparticles. The following examples illustrate the scientific studies that M-STAR will enable.

Topological phase transitions, i.e., the field-induced phase transitions to explore the interaction of topological phases in heterostructures formed by a topological insulator/topological crystalline insulator[41] (e.g., BiSbTe and its family interfaced with SnTe) can be controlled by optical illumination, electric, magnetic, or strain fields. Understanding the spin and magnetic properties with atomic layer resolution of spin textures will enable the study of axion physics[34,42–45] in condensed matter in order to improve our understanding of axions as candidates for dark matter in particle physics. The high intensity of M-STAR will enable experiments of this type since it is highly challenging to achieve a successful gating of the large 1 × 1 cm^2 area required for conventional reflectometers, i.e., MAGREF at the first target station.[25] Optical gating is also typically limited by the spot size of the laser beam and is most effective if the spot remains focused over an area up to mm^2.[39] The combination of PNR with GID of individual monolayers in a superlattice can be used to probe the magnetism in layered antiferromagnets and to study intralayer ferromagnetic exchange.

The GID, magnetic OSS, and GISANS capabilities of M-STAR will all be used to study the fluctuations of magnetic dopants or interface induced magnetic spin textures by antiferromagnetic (AFM) materials and their nonuniformity, which is key to realizing the quantum anomalous Hall effect at room temperature. The study can be extended to the use of two-dimensional graphene, for example, to study the Sachdev-Ye-Kitaev model of a black hole in duality, for which depth resolution is critical.[46] Existing instruments do not have the sub-nanometer depth resolution and monolayer sensitivity required to access the physics of these interfaces. The high intensity and the wide wavelength band of M-STAR, combined with the application of various excitation fields, e.g., electric, optical, magnetic fields, and strain fields, will further open up exciting possibilities for exploring time-dependent processes in thin samples of a few monolayers, such as 2D magnetic and twisted materials.

3. Probing nonequilibrium magnetization dynamics with PNR

The proposed STS instrument M-STAR will provide new capabilities and significantly reduced measurement times that will enable previously impossible nonequilibrium measurements of spintronic materials and devices. By exciting the magnetization dynamics using *in operando* microwave radiation, it will be possible to study the generation of pure spin currents, i.e., the net flow of spin angular momentum without any accompanying charge current. This approach represents a new paradigm in the field of spintronics and offers the potential for novel approaches to store and process information that goes beyond what can be achieved with charge currents. Spintronic devices involve the injection and accumulation of spin at the interface between a ferromagnet and a nonmagnetic material. While we have been able to show proof of principle of this type of measurement at the SNS MAGREF,[47] the new instrument M-STAR will provide a 100-fold gain of the polarized neutrons flux using the focusing mode to enable a quantitative determination of fundamental properties such as the efficiency of spin-pumping and spin accumulation in magnetic heterostructures. The ability to measure the perpendicular component of the static magnetization, provided by the GID geometry, will open new possibilities for studying spintronic materials with perpendicular anisotropy, which play an important role in many spintronic devices, including spin transfer torque magnetic random-access memories, spin torque oscillators, and readout heads for hard drives. For many of these materials, the exact mechanisms responsible for their perpendicular anisotropy remain a subject of discussion. The ability to probe the perpendicular component of the magnetization throughout the heterostructure will provide crucial and new insights that will improve our fundamental understanding. Similarly, the ability to measure the perpendicular component of magnetization will provide vital information about the emergence of an antisymmetric exchange interaction, also known as the Dzyaloshinskii–Moriya interaction (DMI), due to broken symmetry in magnetic thin films. This interaction plays a central role in the formation of skyrmions, i.e., topologically protected states in magnetic materials. In addition, the high flux of polarized neutrons available for the proposed M-STAR will, for the first time, make it possible to characterize the dynamic properties of magnetic materials away from equilibrium. This can be achieved by using microwave radiation to drive the system out of equilibrium, which not only excites spin precession in a ferromagnetic material but also drives a pure spin current into adjacent layers.

4. Functional materials

Functional materials, such as magnetoionic devices, organic/ferromagnetic interfaces, and halide perovskite-based optoelectronics, often require the use of a polarized beam. In these systems, the intensity gains of M-STAR will facilitate accurate characterization of the critical parameters at their interfaces (Fig. 1).

The control of magnetism via electric fields remains an essential objective of low dissipation spintronics development. Magnetoionics is a relatively new field in which voltage drives ion-transport, such as oxygen, lithium, hydrogen, and nitrogen in magnetic materials, to tailor magnetic states in heterostructures reversibly. Magnetoionics holds promising application potential in areas that require endurance and moderate operation speeds, such as neuromorphic computing. Neutrons are sensitive to the involved light ions, and polarized neutrons can also spatially resolve the magnetization distribution. These attributes make neutrons an ideal probe to investigate magnetoionic devices *in operando*, providing critical insights into their operation and degradation mechanisms. However, functional devices often have a small size; therefore, these experiments are notoriously challenging and time-consuming in existing PNR instruments. With the development of M-STAR, ORNL could pioneer in neutron reflectometry applications in this emergent field.

5. From atomic to mesoscopic scale in-plane structures

Many of the above-mentioned novel materials and phenomena are closely related to reduced dimension in at least one direction, which increases the surface-to-bulk ratio and, thus, the

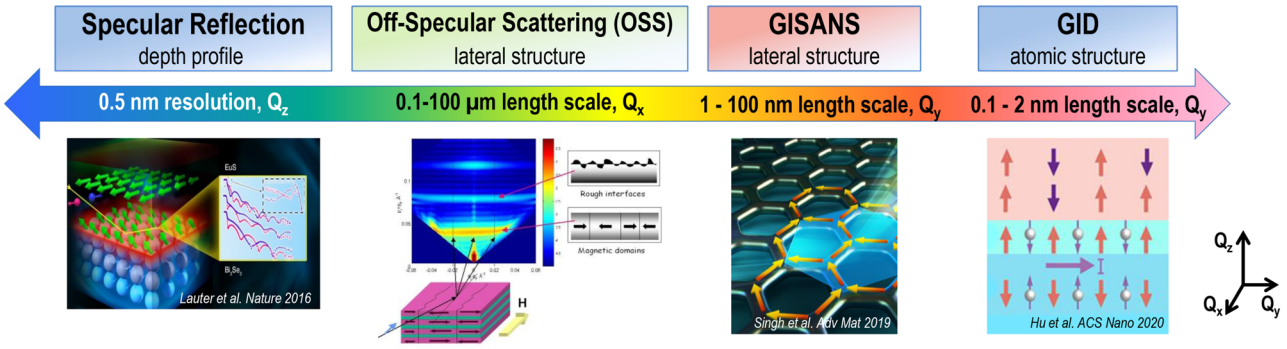

FIG. 1. M-STAR: Four scattering channels. M-STAR will be able to probe a wide spectrum of in-plane scales ranging from a fraction of a nanometer to a few submillimeters. Such unique capability will enable us to establish grazing incidence crystallography addressing various kinds of natural and artificial in-plane structures.[33,48,49] Image illustrating GISANS is reproduced with permission from Adv. Mater. **31**(16), 1808298 (2019). Copyright John Wiley and Sons and Copyright Clearance Center 2022. Image illustrating GID is reproduced with permission from ACS Nano **14**, 12037 (2020). Copyright 2020 American Chemical Society.

role of boundary conditions. Another factor that plays a decisive role in determining the physics of thin films is the particular shape of their boundaries. For example, the presence of extended flat interfaces reduces the effective size of new materials, providing a strong anisotropy of their basic properties, which can differ dramatically from properties of the same bulk material. Moreover, the geometry of thin films can even change their atomic and magnetic structure, i.e., due to the effect of truncation of interfaces that violate the general structural symmetry existing in bulk. This happens particularly in the case of exchange interaction between FM and AFM materials through their common interface, FM layers exchange coupled via non-FM metallic, insulating, or SC thin layers, etc. One can easily enumerate a number of other proximity effects that dramatically change the "bulk" magnetic, electric, or thermodynamic properties. However, there is almost no information on atomic-scale; for example, the evolution of magnetic structure under surface generated fields is available. Such information may be of particular interest, for example, for non-centrosymmetric crystal structures with broken mirror parity, which allows for magnetic chirality. To date, little is known about the relationship between chirality and the underlying crystal lateral structures, for which surfaces and interfaces should play the role of extended defects violating mirror symmetry. Depth-resolved atomic-scale information on in-plane structures will be obtained using the special GID option of the M-STAR instrument at STS. This option will also be used to address magnetic long wavelength structures whose lateral dimensions are much larger than the interatomic distances but smaller than those covered by GISANS or OSS. Hence, M-STAR will be able to explore the entire spectrum of in-plane scales ranging from a fraction of a nanometer to several submillimeters (Fig. 2). This unique capability will enable us to establish grazing incidence crystallography targeting various kinds of natural and artificial in-plane structures composed of nanomagnetic and micromagnetic elements with complex in- and out-of-plane arrangements over flat substrates as exemplified in the GID.

6. Probing dynamics in thin films

It is quite obvious that the possibility to directly probe with GIINS of the excitation spectrum in thin films and multilayers will open up new horizons in those areas of physics where boundary conditions at the interface plays a decisive role. Indeed, the presence of interfaces stratifying thin film materials can prevent modes from propagating across their thickness, which leads to new phenomena due to localized quantum near-surface states substantially altering, for example, their thermodynamic properties.

In particular, the GIINS application will render qualitatively new information on surface spin waves (SWs), a hot topic in view of nanotechnology, and neutron scattering is predestined to investigate their behavior.[30] In the past, neutron scattering has delivered indispensable information on, for example, the SW dynamics of bulk magnetic materials. However, there is a lack of information on near-surface magnons studied with neutrons. Inelastic neutron scattering (INS) from surfaces and thin films is still a challenge. The main reason for this is the lack of high-intensity dedicated reflectometers, although a proof of INS from a thin sample measured in reflection geometry for a supermirror multilayer was demonstrated[31] without energy analysis. One of the problems common to near-surface scattering is that the number of nuclei or spins involved in the scattering process near surfaces is small, and the effective interaction of neutrons with nuclei and atomic spins is relatively weak. Meanwhile, the latter fact, along with low absorption, is usually considered one of the main advantages of neutrons, which penetrate deeply and nondestructively into thick materials. Moreover, due to the weak interaction, neutron scattering can be easily considered in the first order of the perturbation theory, i.e., simply in the Born approximation (BA), which provides a fairly accurate theoretical description of the scattering cross section, which is almost independent of the shape of the sample and the boundary conditions on its surfaces. However, this is not always the case, in particular, when one of the large surfaces of the sample is flat and a well-collimated neutron beam impinges on it at shallow angles. Then, near-surface atoms scatter neutron waves almost coherently in the SR direction with small phase shifts relative to the wave incident on the surface. Consequently, due to constructive interference of the incident and scattered waves, the neutron field near the surface is noticeably enhanced, partially compensating for the lost scattering volume.

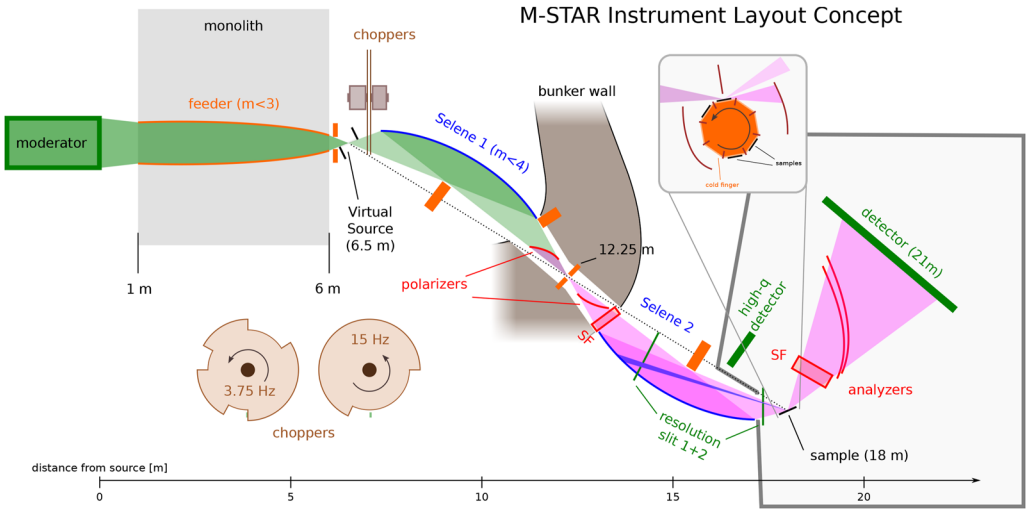

FIG. 2. A diagram of the M-STAR beamline layout and its components. The Selene optics recreates the neutron beam at the sample position (18 m) as defined by the virtual source that is positioned at 6.5 m from the neutron moderator. Defining the footprint far away from the sample has the advantage that only neutrons that are going to touch the sample are transported.

Therefore, reflection geometry can provide access to the INS, both nuclear and magnetic, sensitivity to dynamics in the surface layers. However, grazing incidence inelastic surface scattering (GIINS) enhanced by interference effects cannot be described in BA, and by analogy with elastic OSS, GISANS, or GID, the distorted wave Born approximation (DWBA) must be used. The interference effects taken into account by the DWBA will add up to two orders of magnitude in intensity, as shown in a reflectometry experiment.[50] An additional increase in the ISS intensity is achieved due to the small incoming scattering angle, which provides a noticeably extended footprint of the sample compared to the actual thickness of the surface layer or multilayer. M-STAR will be the world's first reflectometer with a dedicated option to probe surface and/or thin film dynamics under gazing incidence. This development will open doors for the study of surface spin waves in continuous FM and AFM films and multilayers, modes of magnetic excitations in Skyrmion lattices, coherent switching modes in magnetic nano-valves arranged into lateral lattices (mRAM), domain wall propagation in nanowires and micro-wires, and Doppler shift (racetrack memory concept).

II. M-STAR DESIGN AND PERFORMANCE

A. High-level capability requirements

The key capabilities of M-STAR are determined by the scientific challenges described in Sec. I B. The main characteristics are high intensity, low background, broad wavelength band, and small samples. This implies that the overall length of the instrument must be rather short and that the instrument should be equipped with advanced focusing optics. M-STAR will operate at 15 Hz and at hybrid pulse-skipping option at 3.75 Hz to achieve a relative q-range coverage of a factor of 10. M-STAR will be equipped with polarized neutrons and polarization analysis. A second position-sensitive detector for GID is foreseen. The GIINS operating mode is a dedicated advanced capability based on ToF OSS, ToF GISANS, or ToF GID. It will provide depth-sensitive inelastic scattering inherent for reflectometry. A fast chopper in front of the sample is foreseen.

B. Instrument description

M-STAR is a reflectometer that allows specular measurement on tiny samples using the focusing reflectometry technique.[25] In contrast to conventional reflectivity, the resolution for the reflection angle is not provided by collimation before the sample but from the detector, allowing large divergent beams to be used for significant gain factors in intensity. Several newly built instruments are already employing this approach, including the upgraded reflectometer AMOR at PSI[51,52] and CANDOR at NIST,[53] and it will also be utilized by the ESTIA beamline at the ESS.[54] Starting from 1 m after the moderator, the neutron beam is guided within the monolith insert using a straight to parabolic focusing neutron guide to a virtual source (VS) slit at a distance of 6.5 m from the moderator. The heavy collimation setup will be installed between the exit window of the monolith vessel and the VS to suppress fast neutrons, limiting the size of the transmitted beam to only 10×20 mm^2. The parabolic feeder in the monolith not only leads to small reflecting angles and homogeneous illumination of the VS but also provides a much smaller opening of the inner shielding layer compared to, e.g., ESTIA at ESS, which will reduce background and shielding requirements. Downstream of the VS, two bandwidth choppers will be placed: one standard 15 Hz disk with ~115° opening angle for standard operation and a 3.75 Hz hybrid pulse-skipping chopper that allows two full and one double band pulses to be transmitted before blocking every fourth pulse entirely (Fig. 3).

The VS is defined by a slit system that can be rotated to allow cutting the beam into a shape that corresponds to the shape of a rectangular sample under a small angle. This shaped beam is then

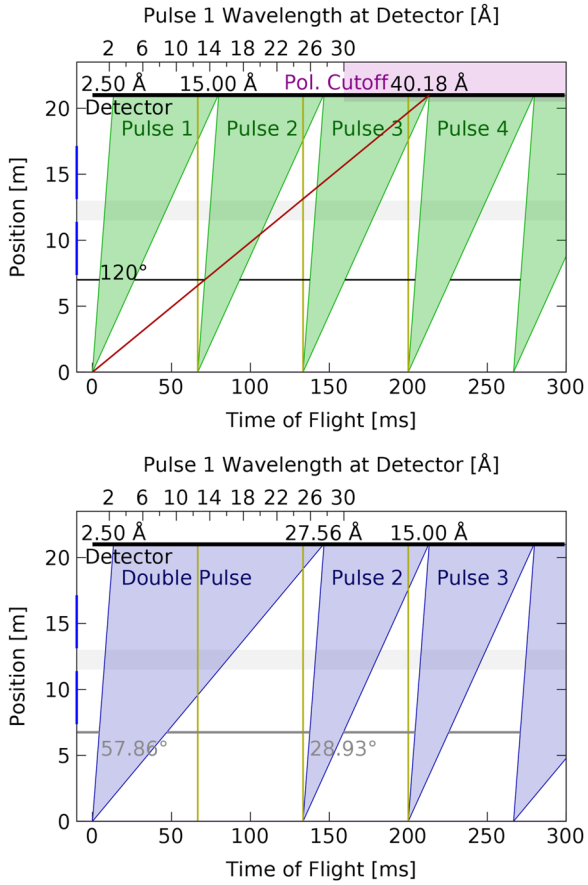

FIG. 3. ToF–distance diagram of standard (top) and hybrid (bottom) chopper operation modes.

projected onto the sample surface through the Selene neutron guide,[54] similar to an image behind a lens. For a perfect guide, this would allow the transport of all neutrons that can interact with the sample surface in the experimental cave while also removing neutrons that cannot interact with the sample, reducing background requirements and increasing the signal-to-noise ratio. Given the typical manufacturing tolerances of state-of-the-art neutron optics, the focus at the sample will be blurred by about 0.25 mm, which leads to a fraction of unused neutrons that depends on the sample size and incident angle. The Selene neutron guide[55] consists of two elliptical neutron guide sections with a reflector at the top/bottom and left/right, respectively. The ellipse refocuses the beam from the VS back to a middle focus, which is distorted due to geometrical aberration effects. The second ellipse, by symmetry, corrects for these aberrations, recovering the shape of the VS slit at the sample position. In the M-STAR layout, the first ellipse is inside the neutron bunker and the second ellipse is outside the bunker wall. At the end of each ellipse, the direct line of sight to the upstream focus is lost. Thus, the high energy neutrons and gamma rays already reduced with heavy collimation before the VS are strongly suppressed before leaving the bunker enclosure. The proposed geometry of the guide will allow 1.4° of beam divergence to be transported in both directions. The Selene guide of M-STAR is optimized for shorter wavelengths, leading to a broader relative wavelength band that can be used efficiently due to the relatively short pulse of the STS source. Neutron guide coatings can be moderate, with the maximum required m-values being below 4. Between the two guides, two curved logarithmic spiral transmission polarizers are inserted for efficient spin selection, reaching the expected spin-polarization of >98% over the entire wavelength band (2.6–15 Å). Details on how these logarithmic spiral polarizers work and their expected performance at longer wavelengths can be found in Ref. 56. They perform as theoretically expected from the coating quality. The AMOR upgrade included a double transmission polarizer that is also consistent with the expected quality.[68,69] We, therefore, base our expected polarization on commercially available transmission supermirror coatings (see, e.g., SwissNeutronics m = 5 transmission polarizer[58]) that can polarize a large wavelength band. These mirrors also filter very long wavelength neutrons (frame overlap). For unpolarized operation, one mirror can be replaced by an uncoated substrate that does not affect the selected wavelength band.

After the second guide section, the beam enters the experimental cave and hits the sample at the focus location, while a position-sensitive detector located at 3 m after the sample records the neutron events. The resolution for off-specular scattering and GISANS is produced by a slit before the sample after which no further reflection can occur. The slits are shown in Fig. 2, marked as "resolution slit 1 + 2." Any potential off-specular or GISANS scattering in the Selene mirrors may blur the beam size at the sample and could potentially increase the background effects. Current supermirrors, however, have been shown to have negligible scattering, several orders of magnitude below the specular reflection. The detector requires a relatively high spatial resolution (~1 mm) coupled with an ability to handle high count rates, which can be achieved by the multi-blade ^{10}B,[56] GEM,[59] or a scintillator base detector, such as the SoNDe concept.[60] The second detector in a fixed position or a separate arm at a distance of about 2 m from the sample will allow for GID and WAD experiments to study atomic structures of thin films. Two high-performance curved logarithmic spiral transmission polarization analyzers (P > 98%) for reflected and diffracted beams will be available for reflection and diffraction operational modes of the instrument.

A dedicated cryomagnet with a vacuum chamber and rotatable cold finger will allow for low background and fast measurements on several samples within a broad temperature range. For GID, a miniature sample mover for precise alignment of the crystal lattice will be attached to the cold finger, either hexapod or piezo stages may be used. This geometry benefits from the fact that the focused beam is symmetric, allowing similar collimation in both the horizontal and vertical directions. The presented layout will allow to build a continuous vacuum from before the VS to the sample and absorb the transmitted beam inside the vacuum chamber. This will not only reduce the beam losses due to scattering but also eliminate various sources of background. Downstream of the sample is an absorbing flight tube with He, which will shield the detector from ambient background and reduce losses between the sample and the detector.

1. Fast chopper

The inelastic capabilities using a fast chopper require that the instrument is situated at the cylindrical moderator with significantly shorter pulses. The FWHM of the STS pulse at the cylinder/tube moderator is 80/170 μs at 3 Å and 200/300 μs at 10 Å, respectively. For the best achievable resolution, it can be considered that the chopper can generate an infinitely short pulse at the sample position. The pulse length on the detector is the pulse length PL*3m/(21-3)m (for a sample–detector distance of 3 m). The ToF from the sample to the detector corresponds to 2.3/7.6 ms for 3/10 Å respectively. This leads to a relative energy resolution at the elastic line of 0.6%/1.3% at 3 Å and 0.4%/0.7% at 10 Å.

Converting into energy resolution results in 108/232 μeV at 3 Å and 6.5/11.3 μeV at 10 Å. This is obviously the highest achievable resolution limit at zero intensity. Considering that the optimal working resolution will have a pulse length similar to the source, the resulting resolution will be about four times higher than the values given above. A compact 100 Hz chopper close to the sample position should be easy to install by and place in this position. The closing/opening time of such a system would be 80 μs, any decrease in divergence angle or increase in frequency will linearly decrease this time.

C. Key characteristics of the instrument concept

The layout of the M-STAR instrument (Fig. 4) is optimized for three main characteristics: low instrument background, large bandwidth, and small samples. A large bandwidth is achieved by the short moderator to detector distance of 21 m, allowing a usable band of neutron bandwidth of 11.8 Å. With the hybrid pulse-skipping option described below, this will be expanded to about 23 Å for a relative q-range coverage of a factor of 10. Polarized measurements will be restricted to a bandwidth of 11.8 Å due to the intrinsic limitations of the Fe/Si supermirror coatings of the devices.

Selene optics deliver a symmetric beam with the ability for vertical and horizontal collimation. The focusing is done in 2D with a vertical cross section that is equal to the horizontal one, as shown in the instrument sketch (see Fig. 4 for a 3D view). The geometrical shape precision required is in the order of 5×10^{-5} rad to produce a focus of better than 0.5 mm, within the proven manufacturing capabilities of neutron guide suppliers.

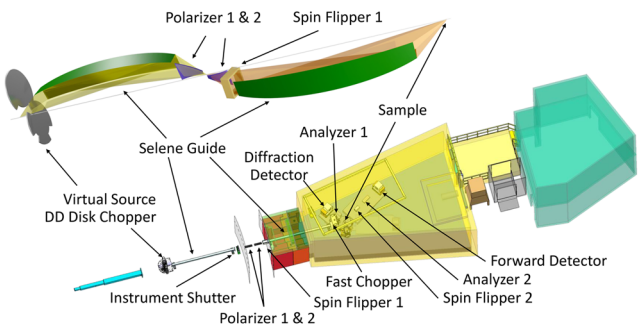

FIG. 4. Conceptual beamline layout of M-STAR showing the placement of key components.

The ability to measure tiny samples down to 2 × 2 mm^2 is made possible by a truly focusing neutron guide and the use of the full divergence for specular reflectivity. This technique uses the fact that specular reflectivity has the same reflecting and incidence angle; thus, the reflection angle can be determined from the beam position on the detector. For typical sample sizes of 10 × 10 mm^2, this technique can also be used to achieve unprecedented counting times of a few seconds instead of the typical hour for equivalent measurements on MagRef/BL-4A at the FTS (see comparison in Fig. 5).

Several aspects of the beamline optics also facilitate a low intrinsic instrument background. The exit window of the neutron feeder at the outer face of the monolith is just 25 × 15 mm^2, drastically reducing the number of fast neutrons leaving the target area into the beamline. Copper substrates will be used to optimally employ the guide boundaries for shielding purposes and to prevent degradation of the inner guide as has been seen at other facilities for the in-pile optics with glass substrates.[61] After passing through the virtual source (VS), the beam is reflected both horizontally and vertically out of line of sight of the moderator before reaching the bunker wall. The remaining fast neutrons scattered by the guide are further restricted by a 40 mm diameter copper collar at the middle focal point 12.25 m from the moderator as well as by another line-of-sight avoidance setup present in the second ellipse of the Selene guide. Beam collimation will be done within the guide at 3 m from the sample and a second slit at the guide exit (see Fig. 2, Slit 1 and Slit 2) will prevent any scattered neutron from entering the cave. Another factor is the focusing of the beam itself; in contrast to a conventional neutron guide with the same divergence, which after entering the cave is collimated to the desired divergence and size, the Selene guide transports three orders of magnitude fewer neutrons with the same intensity hitting the sample surface. Finally, a continuous vacuum from the beginning of the neutron bunker to the sample position minimizes neutron loss and scattering. The cryogenic vacuum for the sample is separated from the rough beamline vacuum only by a micrometer thin aluminum foil. The direct beam passing the sample is then absorbed before leaving the vacuum vessel. For alternative

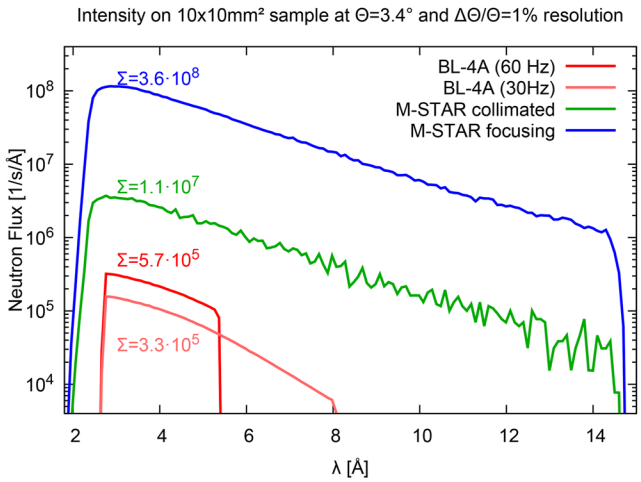

FIG. 5. Comparison of MagRef (BL-4A) on FTS with M-STAR in different operation modes.

sample environments, this last section can be replaced by a sapphire window and a short in-air flight path Table I.

D. Expected performance

Neutron ray tracing simulations have been conducted for the M-Star instrument using the McStas[62] software with the STS tube moderator (differences with the cylindrical moderator were minor). The model included the feeder, VS, and Selene guide optics as well as a square sample modeling a Ni thin film on silicon. Events were recorded at the detector and then processed using their time-of-flight information to reconstruct the sample reflectivity and to get the expected neutron intensity for each q-bin. The results for the simulation are shown in Fig. 6 for a modeling with focusing mode on 10 × 10 and 2 × 2 mm^2 samples, as well as with conventional collimated mode of $\Delta\Theta/\Theta$ = 1%. Experiments with tiny samples can be done in less than an hour, even with additional intensity losses for polarization. For standard 10 × 10 mm^2 samples, a full reflectivity measurement is feasible within just a few seconds and for a moderate q-range, while the hybrid pulse-skipping chopper can make conducting dynamic experiments in just a few seconds resolution feasible. Even in the standard collimated mode, the expected intensity is sufficient to perform full polarization analysis experiments in less than an hour.

E. M-STAR grazing incidence diffraction (GID) option

M-STAR will be installed at a high brilliance neutron source, the second target station at the SNS, and will provide fast recording PNR curves from small samples over a wide range of 1D

TABLE I. Primary M-STAR instrument components and their locations.

Component	Description	Location from moderator (m)
	Beam extraction and shaping	
Feeder optics	In-pile neutron guide for beam extraction	0.9
Heavy collimator 1	Shielding block with pin-hole to scatter fast neutrons	6.1
Virtual source	Five-axis slit system to define beam footprint at sample	6.5
Bandwidth chopper	Two disks @ 15 Hz	6.8
	Beam delivery	
Selene 1 vacuum	Large chamber containing Selene optics and support carrier	7.2–10.4
Selene 1 support	Long structure within vacuum to support and align the optics	7.2–10.4
Selene 1 optics	Highly accurate elliptical reflectors	7.2–10.4
Heavy collimator 2	Shielding block to block fast neutron direct view	9
Heavy collimator 3	Shielding collar around beam containing path through wall	10.4
Instrument shutter	Light shutter to close cold beam	11.4
Bunker wall vacuum	In-wall vacuum vessel for middle-focus components	10.5–13
Polarizer 1	Transmission supermirror polarizer (logarithmic spiral) + FOM (frame overlap mirror)	11.5
Heavy collimator 4	Shielding collar around beam containing path through wall	12.25
Polarizer 2	Second polarizer for improved polarization	13
Spin-flipper 1	RF neutron spin-flipper to select incoming polarization	13.5
Guide shielding	Concrete/steel shielding for open neutron guide path	13.5–15.5
Selene 2 vacuum	Large chamber containing Selene optics and support carrier	14–17.2
Selene 2 support	Long structure within vacuum to support and align the optics	14–17.2
Selene 2 optics	Highly accurate elliptical reflectors	14–17.2
Resolution slit	Four-axis slit system for angular resolution (in vacuum)	14.5
Heavy collimator 5	Shielding block to block fast neutron direct view	15.5
	End station	
Background slit	Four-axis slit system removing scattering background	17.5
Experimental cave		15.5–25.5
Fast chopper	Small 1 disk @ 100Hz	17.8
Sample position		18
Spin-flipper 2	RF neutron spin-flipper to select outgoing polarization	18.5
Analyzer 1	2× transmission supermirror analyzer	19
Analyzer GID	Supermirror analyzer	20
Forward detector	PSD for reflectometry and GISANS	22
Diffraction detector	PSD for GID	21

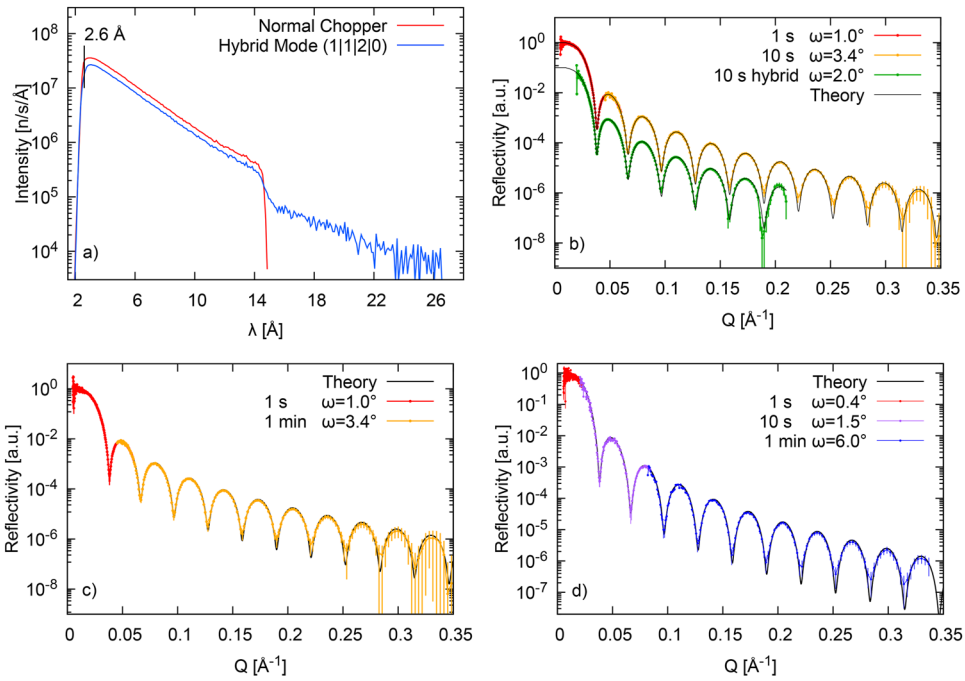

FIG. 6. McStas simulations for M-STAR. (a) ToF flux at the sample position for two operational modes at 15 Hz (red solid line) and 3.75 Hz hybrid pulse-skipping chopper that allows two full and one double band pulses (blue solid line); (b) simulated reflectivity for Ni film 10 × 10 mm^2 for two operational modes at 15 and at 3.75 Hz and the corresponding measuring time; (c) simulated reflectivity for a 2 × 2 mm^2 sample; (d) simulated reflectivity for a 10 × 10 mm^2 sample and neutron beam with the wavelength band of 4–16 A and collimated beam with Δq/q = 1%. ω denotes the incident angle α for the center of the used divergence; for the focusing mode simulations, the divergence is ±0.7°, and for the collimated mode simulations, it is 0.01* ω.

wavevector transfer variation. This range will be extended from the total reflection region to inverse interatomic distances. The latter scales are usually accessible with conventional 3D diffractometry operating in the "wide-angle" mode of atomic diffraction. In contrast, the former ones are readily probed with reflectometry, with its extreme sensitivity to near-surface and interfacial phenomena as well as to SLD distribution across thin film thickness. Such sensitivity is absent in conventional diffractometry and cannot be compensated for by its ability to provide information on the 3D atomic and magnetic arrangement, averaged over the bulk of the films and independent of the boundary conditions at the surfaces and interfaces. On the other hand, SR measures the mean SLD value averaged over in-plane distances within a coherence ellipsoid and summed incoherently over different ellipsoids totally covering the sample volume. The coherence volume is usually quite small, but at grazing incidence, it is extremely anisotropic. Usually, SR is measured at fine out-of-plane but relaxed in-plane collimation. The OSS from the deviations in SLD from its mean value readily allows measuring the Bragg diffraction from artificial in-plane structure with periods ranging from 100 nm to dozens of micrometers. Smaller scales are accessible in GISANS, which require 2D collimation of the incident beam.

All these options are standard for conventional reflectometers and will be substantially improved and implemented in the design of the M-STAR instrument. The solution to access the in-plane atomic-scale structures with the depth sensitivity typical for SR implemented in the M-STAR reflectometer design is a new option specialized for measurements of the grazing incidence lateral diffraction. This option will combine diffractometry with reflectometry using the same beam-forming and polarization setup, the advantages of ToF mode, as well as depth sensitivity. M-STAR will be equipped with one or more additional position-sensitive detectors placed at lateral diffraction angles in the horizontal plane. GID combines optical effects near the critical edge (reflection/refraction) with in-plane Bragg scattering, so it is related to conventional diffraction in the same way that GISANS is related to conventional SANS and offers similar advantages of surface sensitivity and signal enhancement. The layout of the instrument including the GID detector is shown in Fig. 7 (top), and the scattering geometry of the GID experiment is depicted in the bottom of Fig. 7.

In view of the remarkable possibilities provided by GID, it is also important to note that out-of-plane magnetization is not accessible in conventional reflectometry. M-STAR will make it accessible. One of the key properties of GID that complements PNR and OSS is its sensitivity to the direction of the magnetic moment normal to the surface. This property is essential for studying systems with perpendicular anisotropy as well as with an antiferromagnetic structure. Another important property is that the coherence length for GID reduces in any direction to the value of the order λ/Δω (where ω is azimuthal angle), which is much smaller than the characteristic size of ferromagnetic domains. This means that GID is a kind of local probe for domain magnetization: The diffraction intensity of each individual domain adds up incoherently. A feasibility of GID to study the multi-domain state in ferromagnetic films was demonstrated in pilot experiments.[29] This confirmed theoretical expectations and sufficient luminosity of the method.

F. M-STAR grazing incidence inelastic scattering (GIINS) option

Neutron spectroscopy is recognized as one of the most powerful tools to probe atomic and spin dynamics in condensed matter,

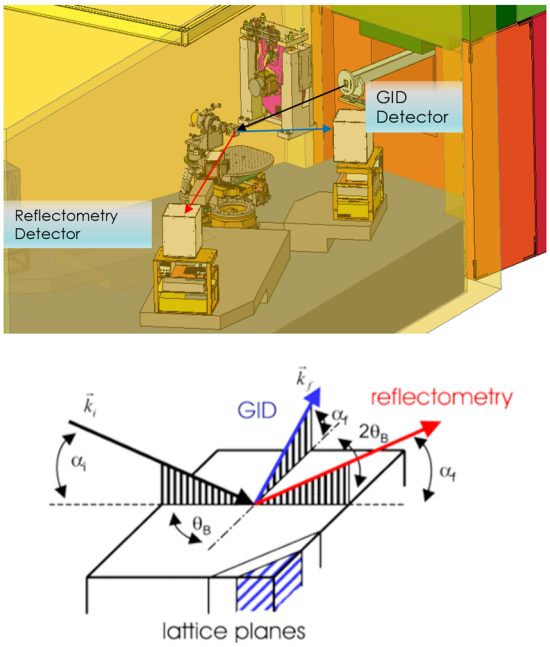

FIG. 7. Sketch of M-STAR in GID scattering mode (top) and the corresponding scattering vectors on the sample that illustrate the relevant Bragg plane and angles (bottom).

providing detailed and fundamental information over a wide range of scales in time and space. This became possible due to the large number of different types of spectrometers available at all the leading neutron facilities in the world. At the same time, there are practically no instruments dedicated to probe the dynamics of surfaces and/or thin films, both intrinsic and induced by an external time-dependent field. Meanwhile, a few recent experiments carried out on, e.g., lipid bilayers stacked into periodic multilayers unambiguously demonstrated the ability of neutron triple-axes spectroscopy to address some questions on the co-operative dynamics of biomimetic membranes.[32] Despite the success of these experiments, it should be recognized that this type of spectrometry is not an ideal method to study the dynamics of surfaces and thin films due to its relatively low luminosity. It this respect, a dedicated advanced option based on ToF OSS, ToF GISANS, or ToF GID will not only be more efficient, but it will also provide the significant depth sensitivity intrinsic for reflectometry. Indeed, in Ref. 63, it has been shown that ToF OSS can be easily observed from a single lipid bilayer in equilibrium and quantitatively described in the DWBA approach by the model of thermally excited capillary waves. The experiments were carried out on the reflectometer (SPEAR) at the Los Alamos Neutron Science Center in the ToF mode but without analysis of the energy transfer of scattered neutrons. Therefore, only the OSS signal integrated over energy transfer was available for theoretical interpretation, without direct proof of its inelastic origin. This does not allow us to unambiguously confirm the model and determine the range of its applicability. A chopper inserted close to but before the sample and measurement of the neutron flight path from the sample to the detector will allow for (1) a clear discrimination of the inelastic contribution from the inelastic counterpart and (2) further investigation into the excitation spectrum by tracing the inelastic signal over the PSD. The main advantage of this method is the active use of the time structure of the incident beam, which, together with an additional chopper, can provide an accuracy of determining the energy transfer up to 1%. Another advantage is that at each energy transfer value ω, a complete 2D data map is simultaneously recorded as a function of λ and α_f. This map can be converted into lateral and transverse wavevector transfers, while the precision ω measurements can reach 1% in accordance with the accuracy of the wavelength.

It is obvious that the possibility of a direct study of the excitation spectrum in thin films and multilayers using GIINS will open up new prospects in those areas of physics where boundary conditions at interfaces play a decisive role. Indeed, the presence of interfaces separating thin film materials can prevent modes from propagating though their thickness, which leads to new phenomena due to the fact that localized quantum near-surface states change significantly, for example, their thermodynamic properties.

In particular, GIINS application will render qualitatively new information about surface spin waves (SWs), which is a hot topic in view of nanotechnology, and neutron scattering is predestined to investigate their behavior.[64] Inelastic surface scattering (ISS) enhanced due to interference effects cannot be described in BA and the DWBA must be used by analogy with elastic OSS, GISANS, or GID.[65–67] The interference effects, taken into account by the DWBA, will add up to two orders of magnitude of intensity, which has been shown to be accessible in the reflectometry experiment.[30] An additional increase of the ISS intensity is achieved due to the small angle of incoming scattering, providing an appreciably extended footprint of the sample compared to the actual thickness of the surface layer or of a multilayer. With an additional chopper, M-STAR will also be able to analyze the energy transfer of GID providing access to AFM SWs.

1. M-STAR ToF spectroscopy setup

In the proposed M-STAR setup for ToF spectroscopy, a fast chopper directly in front of the sample determines a series of short pulses with a wavelength defined by the moderator to chopper flight time while the outgoing wavelength is determined by the sample to the detector flight time. The layout of the proposed setup is shown in Fig. 8.

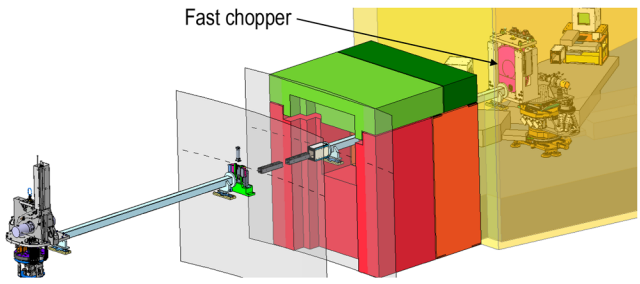

FIG. 8. Sketch of M-STAR in GIINS scattering mode; a compact fast chopper close to the sample location defines a series of short pulses.

The accessible energy resolution depends on the incident wavelength and the energy transfer and, in general, gets better toward energy loss scattering. With the planned instrument and source parameters, the resolvable minimum energy transfer at 3/10 Å would be 120/7 μeV for the cylinder and 230/11.3 μeV for the tube moderator. The highest measurable energy loss is primarily defined by the incident neutron energy, in these examples ~50/~10 meV.

The advanced polarized neutron reflectometer M-STAR with the development of novel GID and GIINS operation modes in ToF will open up a new terrain for the field of neutron scattering. It will become a powerful and unprecedented tool with great versatility to address a plethora of important and fascinating aspects in nanoscience, related to the structural, magnetic, dynamic, and kinetic properties of thin film heterostructures and surfaces.

III. CONCLUSIONS

The low repetition rate and increased brightness of the STS peak are ideal for designing new generation polarized neutron reflectometers. The low repetition rate allows for a broad wavelength band necessary to obtain a broad q-range at one incident angle and to perform experiments at a constant geometry of the sample. Another advantage is the large incident angle for spatial separation of the reflected and direct beams, which provides low background and high angular resolution at small momentum transfers. Advanced focusing optics will increase the instrument performance gain by two orders of magnitude or more. The focusing optics, optimized for very small samples of only a few mm^2, will allow measuring these tiny samples over a wide q-range. The high intensity will allow the development of advanced ToF GID and GIINS capabilities that have not been achieved in the existing neutron reflectometers. Collectively, these advances will dramatically expand the realm of the scientific problems that will be explored with M-STAR, making a transformative impact on developments and applications in science and technology.

ACKNOWLEDGMENTS

We thank Cristina Boone, William Turner, and Scott Dixon for their attention and help during the development of the beamline layout and its key components and Bill Mchargue for useful discussions on the choppers. We thank Claudia Mewes, Rana Ashkar, and Kumar Rajeev for their input during the initial stage of the project. This research used resources at the SNS and the HFIR, which are DOE Office of Science User Facilities operated by the Oak Ridge National Laboratory (ORNL). This research used resources of the Spallation Neutron Source Second Target Station Project at ORNL. ORNL is managed by UT-Battelle LLC for DOE's Office of Science, the single largest supporter of basic research in the physical sciences in the United States. This manuscript has been authored by UT-Battelle, LLC under Contract No. DE-AC05-00OR22725 with the U.S. Department of Energy. The United States Government retains and the publisher, by accepting the article for publication, acknowledges that the United States Government retains a non-exclusive, paid-up, irrevocable, worldwide license to publish or reproduce the published form of this manuscript, or allow others to do so, for United States Government purposes. The Department of Energy will provide public access to these results of federally sponsored research in accordance with the DOE Public Access Plan (http://energy.gov/downloads/doe-public-access-plan).

AUTHOR DECLARATIONS

Conflict of Interest

The authors have no conflicts to disclose.

Author Contributions

Valeria Lauter: Conceptualization (equal); Supervision (equal); Writing – original draft (equal); Visualization (equal); Writing – original draft (equal); Writing – review & editing (equal). **Kang Wang**: Conceptualization (equal). **Tim Mewes**: Conceptualization (equal); Writing – original draft (equal). **Artur Glavic**: Conceptualization (equal); Visualization (equal); Writing – original draft (equal); Writing – review & editing (equal). **Boris Toperverg**: Conceptualization (equal); Formal analysis (equal). **Mahshid Ahmadi**: Writing – original draft (equal). **Badih Assaf**: Writing – original draft (equal). **Mingda Li**: Writing – original draft (equal). **Xinyu Liu**: Writing – original draft (equal). **Yaohua Liu**: Writing – original draft (equal); Writing – review & editing (equal). **Jagadeesh Moodera**: Writing – original draft (equal). **Leonid Rokhinson**: Writing – original draft (equal). **Deepak Singh**: Writing – original draft (equal). **Nian Sun**: Writing – original draft (equal).

DATA AVAILABILITY

The data that support the findings of this study are available from the corresponding author upon reasonable request.

REFERENCES

[1] C. F. Majkrzak, "Neutron reflectometry studies of thin films and multilayered materials," Acta Phys. Pol., A **96**, 81–99 (1999).
[2] J. F. Ankner and G. P. Felcher, "Polarized-neutron reflectometry," J. Magn. Magn. Mater. **200**, 741–754 (1999).
[3] B. P. Toperverg and H. Zabel, "Chapter 6 - neutron scattering in nanomagnetism," Exp. Methods Phys. Sci. **48**, 339–434 (2015).
[4] V. Lauter-Pasyuk, "Neutron grazing incidence techniques for nano-science," Collecti. SFN **7**, s221–s240 (2007). https://www.neutron-sciences.org/articles/sfn/olm/2007/02/sfn2007009/sfn2007009.html.
[5] S. J. Blundell, M. Gester, J. A. C. Bland, H. J. Lauter, V. V. Pasyuk, and A. V. Petrenko, "Spin-orientation dependence in neutron reflection from a single magnetic film," Phys. Rev. B **51**(14), 9395 (1995).
[6] L. O'Brien, M. J. Erickson, D. Spivak *et al.*, "Kondo physics in non-local metallic spin transport devices," Nat. Commun. **5**, 3927 (2014).
[7] Q. L. He, X. Kou, A. J. Grutter *et al.*, "Tailoring exchange couplings in magnetic topological-insulator/antiferromagnet heterostructures," Nat. Mater. **16**, 94–100 (2017).
[8] J. Wu, V. Lauter, H. Ambaye, X. He, and I. Božović, "Search for ferromagnetic order in overdoped copper-oxide superconductors," Sci. Rep. **7**, 45896 (2017).
[9] L. Petridis, H. Ambaye, S. Jagadamma, S. M. Kilbey, B. S. Lokitz, V. Lauter, and M. A. Mayes, "Spatial arrangement of organic compounds on a model mineral surface: Implications for soil organic matter stabilization," Environ. Sci. Technol. **48**(1), 79 (2013).
[10] A. Y. Tronin, C. E. Nordgren, J. W. Strzalka, I. Kuzmenko, D. L. Worcester, V. Lauter, J. A. Freites, D. J. Tobias, and J. K. Blasie, Langmuir **30**(16), 4784–4796 (2014).

[11] V. Lauter-Pasyuk, H. Lauter, G. Gordeev, P. Müller-Buschbaum, B. P. Toperverg, W. Petry, M. Jernenkov, A. Petrenko, and V. Aksenov, "Parallel and perpendicular lamellar phases in copolymer–nanoparticle multilayer structures," Physica B **350**(1–3), E939–E942 (2004).
[12] T. L. Meyer, A. Herklotz, V. Lauter, J. W. Freeland, J. Nichols, E.-J. Guo, S. Lee, T. Z. Ward, N. Balke, S. V. Kalinin, M. R. Fitzsimmons, and H. N. Lee, "Enhancing interfacial magnetization with a ferroelectric," Phys. Rev. B **94**, 174432 (2016).
[13] J. Nichols, X. Gao, S. Lee, T. L. Meyer, J. W. Freeland, V. Lauter, D. Yi, J. Liu, D. Haskel, J. R. Petrie, E.-J. Guo, A. Herklotz, D. Lee, T. Z. Ward, G. Eres, M. R. Fitzsimmons, and H. N. Lee, "Emerging magnetism and anomalous Hall effect in iridate–manganite heterostructures," Nat. Commun. **7**, 12721 (2016).
[14] M. D. Biegalski, Y. Takamura, A. Mehta, Z. Gai, S. V. Kalinin, H. Ambaye, V. Lauter, D. Fong, S. T. Pantelides, Y. M. Kim, J. He, A. Borisevich, W. Siemons, and H. M. Christen, "Interrelation between structure - magnetic properties in $La_{0.5}Sr_{0.5}CoO_3$," Adv. Mater. Interfaces **1**, 1400203 (2014).
[15] A. M. Kane, I.-T. Chiu, N. J. Ahlm, R. V. Chopdekar, A. T. N'Diaye, E. Arenholz, A. Mehta, V. Lauter, and Y. Takamura, "Controlling magnetization vector depth profiles of $La_{0.7}Sr_{0.3}CoO_3/La_{0.7}Sr_{0.3}MnO_3$ exchange spring bilayers via interface reconstruction," ACS Appl. Mater. Interfaces **12**, 45437–45443 (2020).
[16] H. Zabel, K. Theis Brohl, M. Wolff, and B. P. Toperverg, "Polarized neutron reflectometry for the analysis of nanomagnetic systems," IEEE Trans. Magn. **44**(7), 1928 (2008).
[17] V. Lauter-Pasyuk, H. J. Lauter, B. Toperverg, O. Nikonov, E. Kravtsov *et al.*, "Magnetic off-specular neutron scattering from Fe/Cr multilayers," Physica B **283**(1-3), 194–198 (2000).
[18] N. Xia, V. Lauter, and R. A. Gerhardt, "Three-dimensional nanoscale mapping of porosity in solution- processed ITO multilayer thin films for patternable transparent electrodes," ACS Appl. Nano Mater. **2**(2), 726–735 (2019).
[19] D. Gorkov, B. P. Toperverg, and H. Zabel, "Artificial magnetic pattern arrays probed by polarized neutron reflectivity," Nanomaterials **10**, 851–872 (2020).
[20] T. Saerbeck, H. Huckfeldt, B. P. Toperverg, and A. Ehresmann, "Magnetic structure of ion-beam imprinted stripe domains determined by neutron scattering," Nanomaterials **10**, 752–774 (2020).
[21] D. Gorkov, B. P. Toperverg, and H. Zabel, "Probing interspatial magnetic flux distributions in ferromagnetic stripe arrays by specular and off-specular polarized neutron scattering," Phys. Rev. B **101**, 224404 (2020).
[22] A. Hafner, P. Gutfreund, B. P. Toperverg, A. O. F. Jones, J. P. de Silva, A. Wildes, H. E. Fischer, M. Geoghegan, and M. Sferrazza, "Combined specular and off-specular reflectometry: Elucidating the complex structure of soft buried interfaces," J. Appl. Crystallogr. **54**, 924–948 (2021).
[23] A. Hafner, P. Gutfreund, B. P. Toperverg, M. Geoghegan, and M. Sferrazza, "2D reectometry for the investigation of polymer interfaces: Off-specular neutron scattering," J. Phys.: Condens. Matter **33**, 364002 (2021).
[24] G. Yumnam, Y. Chen, J. Guo, J. Keum, V. Lauter, and D. K. Singh, "Quantum disordered state of magnetic charges in nanoengineered honeycomb lattice," Adv. Sci. **8**(6), 2004103 (2021).
[25] V. Lauter, H. Ambaye, R. Goyette, W.-T. Hal Lee, and A. Parizzi, "Highlights from the magnetism reflectometer at the SNS," Physica B **404**(17), 2543–2546 (2009).
[26] V. Lauter, H. J. C. Lauter, A. Glavic, and B. P. Toperverg, "Reflectivity, off-specular scattering, and GISANS neutrons," in *Reference Module in Materials Science and Materials Engineering*, edited by S. Hashmi (Elsevier, Oxford, 2016), pp. 1–27.
[27] B. P. Toperverg, "Polarized neutron reflectometry of magnetic nanostructures," Phys. Met. Metallogr. **116**(13), 1337–1375 (2015).
[28] H. Dosch, Critical Phenomena at Surfaces and Interfaces: Evanescent X-Ray and Neutron Scattering, Springer Tracts in Modern Physics (Springer Berlin, Heidelberg, 1992), Vol. 126.
[29] B. P. Toperverg, V. V. Lauter-Pasyuk, H. J. Lauter, and A. Vorobiev, "Grazing incidence neutron diffraction from ferromagnetic films in multi-domain state," Physica B **356**(1-4), 51–55 (2005).
[30] H. J. Lauter and V. Lauter-Pasyuk, "A discussion about inelastic surface scattering," J. Neutron Res. **14**(3), 239–250 (2006).
[31] D. A. Korneev, V. I. Bodnarchuk, V. F. Peresedov, V. V. Zhuravlev, and A. F. Schebetov, "Inelastic mode of polarised reflectometer REFLEX-P for observation of surface phonons and magnons," Physica B **276-278**, 314 (2000).
[32] M. C. Rheinstädter, C. Ollinger, G. Fragneto, F. Demmel, and T. Salditt, "Collective dynamics of lipid membranes studied by inelastic neutron scattering," Phys. Rev. Lett. **93**, 108107 (2004).
[33] F. Katmis, V. Lauter, F. S. Nogueira, B. A. Assaf, M. E. Jamer, P. Wei, B. Satpati, J. W. Freeland, I. Eremin, D. Heiman, P. Jarillo-Herrero, and J. S. Moodera, "A high-temperature ferromagnetic topological insulating phase by proximity coupling," Nature **533**, 513–516 (2016).
[34] Q. L. He, G. Yin, L. Yu, A. J. Grutter, L. Pan, C. Z. Chen, X. Che, G. Yu, B. Zhang *et al.*, "Topological transitions induced by antiferromagnetism in a thin-film topological insulator," Phys. Rev. Lett. **121**(9), 096802 (2018).
[35] K. Chen, A. Philippi-Kobs, V. Lauter, A. Vorobiev, E. Dyadkina, V. Y. Yakovchuk, S. Stolyar, and D. Lott, "Observation of a chirality-induced exchange-bias effect," Phys. Rev. Appl. **12**(2), 024047 (2019).
[36] V. Lauter-Pasyuk, H. J. Lauter, V. L. Aksenov, E. I. Kornilov, A. V. Petrenko, and P. Leiderer, "Determination of the magnetic field penetration depth in $YBa_2Cu_3O_7$ superconducting films by polarized neutron reflectometry," Physica B **248**, 166 (1998).
[37] V. Lauter-Pasyuk, H. J. Lauter, B. P. Toperverg, L. Romashev, and V. Ustinov, "Transverse and lateral structure of the spin-flop phase in Fe/Cr antiferromagnetic superlattices," Phys. Rev. Lett. **89**(16), 167203 (2002).
[38] S. G. Jeong, J. Kim, A. Seo, S. Park, H. Y. Jeong, Y.-M. Kim, V. Lauter, T. Egami *et al.*, "Unconventional interlayer exchange coupling via chiral phonons in synthetic magnetic oxide heterostructures," Sci. Adv. **8**(4), eabm4005 (2022).
[39] M. Wang, H. Xu, T. Wu, H. Ambaye, J. Qin, J. Keum, I. N. Ivanov, V. Lauter, and B. Hu, "Optically induced static magnetization in metal halide perovskite for spin-related optoelectronics," Adv. Sci. **8**, 2004488 (2021).
[40] J. Sclenar *et al.*, "Proximity-induced anisotropic magnetoresistance in magnetized topological insulators," Appl. Phys. Lett. **118**, 232402 (2021).
[41] K. L. Wang *et al.*, MRS Bull. **45**, 373 (2020).
[42] F. Wilczek, "Two applications of axion electrodynamics," Phys. Rev. Lett. **58**, 1799 (1987).
[43] X.-L. Qi, T. L. Hughes, and S.-C. Zhang, Phys. Rev. B **78**, 195424 (2008).
[44] M. Mogi *et al.*, Sci. Adv. **3**(10), eaao1669 (2017).
[45] Chao-Yao Yang *et al.*, "Termination switching of antiferromagnetic proximity effect in topological insulator," Sci. Adv. **6**(33), (2020).
[46] Y. Zang *et al.*, "In-plane antiferromagnetic moments and magnetic polaron in the axion topological insulator candidate EuIn2As2," Phys. Rev. B **101**, 205126 (2020).
[47] T. Mewes, V. Lauter, "Determination of spin accumulation in interlayer exchange coupled trilayers" (unpublished).
[48] Y. Chen, B. Summers, A. Dahal, V. Lauter, G. Vignale, and D. K. Singh, "Field and current control of the electrical conductivity of an artificial 2D honeycomb lattice," Adv. Mater. **31**(16), 1808298 (2019).
[49] G. Hu, Y. Zhu, J. Xiang, T.-Y. Yang, M. Huang, Z. Wang, Z. Wang, P. Liu, Y. Zhang, C. Feng, D. Hou, W. Zhu, M. Gu, C.-H. Hsu, F.-C. Chuang, Y. Lu, B. Xiang, Y.-L. Chueh, "Antisymmetric magnetoresistance in a van der Waals antiferromagnetic/ferromagnetic layered $MnPS_3/Fe_3GeTe_2$ stacking heterostructure," ACS Nano **14**, 12037–12044 (2020).
[50] B. P. Toperverg, "Specular reflection and off-specular scattering of polarized neutrons," Physica B **297**, 160 (2001).
[51] J. Stahn, U. Filges, and T. Panzner, "Focusing specular neutron reflectometry for small samples," Eur. Phys. J. Appl. Phys. **58**, 11001 (2012).
[52] C. Klauser, R. Bergmann, U. Filges, and J. Stahn, "A selene guide for AMOR," J. Phys.: Conf. Ser. **1021**, 012024 (2018).
[53] See https://www.nist.gov/ncnr/chrns-candor-white-beam-reflectometer for description of CANDOR Reflectometer
[54] K. H. Andersen *et al.*, "The instrument suite of the European Spallation Source," Nucl. Instrum. Methods Phys. Res., Sect. A **957**, 163402 (2020).
[55] J. Stahn and A. Glavic, "Focusing neutron reflectometry: Implementation and experience on the ToF-reflectometer Amor," Nucl. Instrum. Methods Phys. Res., Sect. A **821**, 44–54 (2016).
[56] J. Stahn and A. Glavic, "Efficient polarization analysis for focusing neutron instruments," J. Phys.: Conf. Ser. **862**(1), 012007 (2017).
[57] M. Gupta, T. Gutberlet, J. Stahn, P. Keller, and D. Clemens, "AMOR—The time-of-flight neutron reflectometer at SINQ/PSI," Pramana **63**, 57–63 (2004).

[58]See https://www.swissneutronics.ch/products/polarizing-devices/ for Neutron Optical Componenets and Instruments
[59]G. Mauri *et al.*, "Neutron reflectometry with the Multi-Blade 10B-based detector," Proc. R. Soc. A **474**, 20180266 (2018).
[60]See https://n-cdt.com/cascade-2d-200/ for CASCADE Detector Technologies GmbH.
[61]S. Jaksch *et al.*, "Recent developments SoNDe high-flux detector project," JPS Conf. Proc. **22**, 011019 (2018).
[62]R. Boffy, M. Kreuz, J. Beaucour, U. Köster, and F. J. Bermejo, "Why neutron guides may end up breaking down? Some results on the macroscopic behaviour of alkali-borosilicate glass support plates under neutron irradiation," Nucl. Instrum. Methods Phys. Res., Sect. B **358**, 179–187 (2015).
[63]K. Lefmann and K. Nielsen, "McStas, a general software package for neutron ray-tracing simulations," Neutron News **10**(3), 20 (1999).
[64]M. S. Jablin, M. Zhernenkov, B. P. Toperverg, M. Dubey, H. L. Smith, A. Vidyasagar, R. Toomey, A. J. Hurd, and J. Majewski, "In-plane correlations in a polymer-supported lipid membrane measured by off-specular neutron scattering," Phys. Rev. Lett. **106**, 138101 (2011).
[65]B. P. Toperverg, "Introduction to elastic and inelastic neutron scattering at grazing incidence: Advantages of long wavelength in: New methodical developments for GRANIT," C. R. Phys. **12**, 740–741 (2011).
[66]A. I. Okorokov, V. V. Runov, B. P. Toperverg, A. D. Tret'yakov, E. I. Mal'tzev, I. M. Puzei, and V. E. Mikhailova, "Study of spin waves in amorphous magnetic materials by polarized- neutron scattering," JETP Lett. **43**, 503–507 (1986) http://jetpletters.ru/ps/1406/index.shtml.
[67]B. P. Toperverg, V. V. Deriglazov, and V. E. Mikhailova, "On the studies of spin-wave dynamics in amorphous ferromagnets by polarized neutron scattering," Physica B **183**, 326–330 (1993).